Article

Off-Grid Rural Electrification in India Using Renewable Energy Resources and Different Battery Technologies with a Dynamic Differential Annealed Optimization

Polamarasetty P Kumar [1],*, Vishnu Suresh [2,3],*, Michal Jasinski [2] and Zbigniew Leonowicz [2]

1   Department of Electrical and Electronics Engineering, GMR Institute of Technology, Rajam 532127, India
2   Faculty of Electrical Engineering, Wroclaw University of Science and Technology, 50-370 Wroclaw, Poland; jasinski@ieee.org (M.J.); zbigniew.leonowicz@pwr.edu.pl (Z.L.)
3   Hitachi ABB Power Grids Research, ul. Pawia 7, 31-154 Kraków, Poland
*   Correspondence: praveenkumar.p@gmrit.edu.in (P.P.K.); vishnu.suresh@pwr.edu.pl (V.S.)

Abstract: Several families in India live in remote places with no access to grid-connected power supply due to their remoteness. The study area chosen from the Indian state of Odisha does not have an electrical power supply due to its distant location. As a result, this study analyzed the electrification process using Renewable Energy (RE) resources available in the locality. However, these RE resources are limited by their dependency on weather conditions and time. So, a robust battery storage system is needed for a continuous power supply. Hence, the Nickel Iron (Ni-Fe), Lithium-Ion (Li-Ion) and Lead Acid (LA) battery technologies have been analyzed to identify a battery technology that is both technologically and economically viable. Using the available RE resources in the study area, such as photovoltaic and biomass energy resources, as well as the various battery technologies, three configurations have been modelled, such as Photovoltaic Panels (PVP)/Biomass Generator(BIOMG)/BATTERY$_{(Ni-Fe)}$, PV/BIOMG/BATTERY$_{(Li-Ion)}$ and PVP/BMG/BATTERY$_{(LA)}$. These three configurations have been examined using nine prominent metaheuristic algorithms, in which the PVP/BIOMG/BATTERY$_{(Ni-Fe)}$ configuration provided the optimal Life Cycle Cost value of 367,586 USD. Among the all metaheuristic algorithms, the dynamic differential annealed optimization algorithm was given the best Life Cycle Cost values for all of the three configurations.

Keywords: optimization techniques; different batteries; off-grid microgrid; integrated renewable energy system

1. Introduction

Despite the fact that freshwater and energy are essential for human survival, existing and future energy and freshwater demands are having a significant impact on the earth. Renewable Energy (RE) resources play a critical role in addressing these concerns. This is especially true in rural and distant areas where the grid expansion is neither feasible nor cost-effective. For a multitude of reasons, planning and constructing an off-grid microgrid is difficult from a both technological and economic perspective. One of them is the reliance of RE resources on meteorological conditions. A suitable battery storage system is needed for power supply continuity. In order to fulfil the energy requirements, most off-grid systems are either over or under-sized. While the larger system is more expensive and produces more energy, the smaller system is incapable of meeting the required load demands, resulting in a power supply shortage. To overcome these challenges and fully utilize the benefits of an off-grid microgrid built with RE sources, an Energy Management Strategy (EMS) is necessary [1]. Furthermore, renewable energy resources, particularly solar energy resource can be used in a wide range of applications, including solar dryers, solar home systems, solar cookers, thermal power generation and water heaters. The biomass generator can produce both heat and electricity. The hydro energy resource can

be used for irrigation, drinking water supply and hydropower generation. Wind energy has many applications, including power generation, water pumps and windmills. Some commercial and residential applications of battery energy storage systems are explained as follows. From a commercial point of view, battery energy storage systems are useful in the following applications such as peak shaving, emergency backup, microgrids, load shifting, grid services and renewable energy resource integration. From a residential standpoint, battery energy storage systems are useful in the following applications: storing excess energy produced by the solar PV panels, emergency backup and off-grid applications.

Numerous studies on the sizing of microgrids have been published in reputed journals. These approaches can be classified into three broad categories, which are categorized as follows: (i) software tools such as IHOGA, RETScreen, HOMER and HOGA, [2] (ii) deterministic methodologies such as linear programming, numerical, iterative, graphical design, analytical and probabilistic methods [3] and (iii) metaheuristic algorithms such as Grasshopper Optimization Algorithm (GOA), Moth Flame Optimization (MFO), Genetic Algorithm (GA) and Dragonfly Algorithm (DA). Nevertheless, while software tools are simple to use the relevant components inside them cannot be picked. Furthermore, its algorithms and calculations are hidden from users. When it comes to estimating the size of a microgrid, software tools are constrained by certain assumptions. Deterministic approaches, on the other hand, outperform the software tools but the solutions are trapped at the local optima due to its complex design. They are unable to discover the global best optimal values under such conditions. It should be run several times with random beginning conditions to prevent the local optima trapping. Hence, the solution is unlikely to be the global best optimum value. Obtaining the global best optimal solution may necessitate multiple efforts. Finally, metaheuristic algorithms were chosen as the most promising methods, and they are widely used for optimization problems [4].

Last decade, metaheuristic algorithms were built to manage microgrid sizing issues. Surprisingly, certain algorithms, such as Differential Evolutionary Algorithm (DE), Particle Swarm Optimization (PSO) [5] and GA, are well-known among most software engineers as well as other researchers from other disciplines. They are adaptable techniques and offer better results than deterministic methods by preventing the local optima entanglement. These algorithms offer a range of properties that allow them to tackle any optimization problem and they solve optimization problems by imitating natural processes. On the other hand, the No-Free-Lunch theorem states that while a specific metaheuristic algorithm can produce optimal results for a specific objective function, the same algorithm produces lower performance in other objective functions. For such reasons, researchers working on microgrid sizing issues have looked at robust metaheuristic algorithms [6].

A review of the literature on off-grid microgrid size issues revealed that evaluating the techno-economic feasibility analysis with various battery technologies to deliver an uninterrupted electrical supply is quite limited. Moreover, researchers can determine a specific algorithm's robustness and convergence efficiency using various algorithms. However, such studies are limited.

The limitations stated above should be addressed while analyzing perfect off-grid rural electrification from a techno-economic perspective. So, taking these limitations into account, some research has been undertaken to supply power to four un-electrified villages in the Indian state of Odisha. After conducting some research in the study area, it was discovered that the accessible RE resources in the study area are solar and biomass. Solar energy is the most volatile of the two RE resources due to its time-dependent nature and weather conditions. So, the power supply is not continuous. Hence, a robust battery system is essential to ensure a continuous electrical supply. Therefore, in this study, a detailed analysis with three v kinds of batteries, such as Ni-Fe, Li-Ion and LA, has been carried out. Three types of configurations are modelled using available RE resources and battery technologies to identify the most viable configuration for electrifying the study region, such as Photovoltaic Panels (PVP)/ Biomass Generator (BIOMG)//BATTERY$_{(Ni-Fe)}$, PVP/BIOMG/BATTERY$_{(Li-Ion)}$ and PVP/BIOMG/BATTERY$_{(LA)}$. In order to find out a

feasible configuration to electrify the study area, nine proven metaheuristic algorithms have been used in the study, such as Differential Evolutionary Algorithm (DE) [5], Genetic Algorithm (GA) [6], Moth Flame Optimization (MFO) [7], Dragonfly Algorithm (DA) [8], Particle Swarm Optimization (PSO) [9], Ant Lion Optimization (ALO) [10], Grey Wolf Optimization (GWO) [11], Grasshopper Optimization Algorithm (GOA) [12] and Dynamic Differential Annealed Optimization Algorithm [13]. Finally, after identifying the optimal configuration, it is evaluated with various loss of power supply probability values.

The novelty in this work can be summarized as:

- A renewable energy-based plan for electrification of an un-electrified village in a remote location.
- Identification of a suitable optimization algorithm amongst nine prominent ones in the literature for energy management.
- Exploration of the most cost-effective and technically suitable battery storage technology for the given setup.
- Identify the best configuration cost wise amongst three different possibilities.

2. The Study Area Identification

The study examined the off-grid rural electrification procedure using an off-grid remote rural area located more than 50 km away. Power supply to this area via grid connection is not possible due to the area's hilly terrain and its location in the middle of a dense forest. Four villages are included in the study area, which are located in the Chandrapur block of the Rayagada district of Odisha state in India. Figure 1 depicts the study area's location on a map of India. The study area's latitude and longitude are 19.5927° N and 83.8712° E, respectively. The whole population of the villages is accommodated in 153 houses. People in this area continue to rely on candles, kerosene lanterns and solar lamps for illumination.
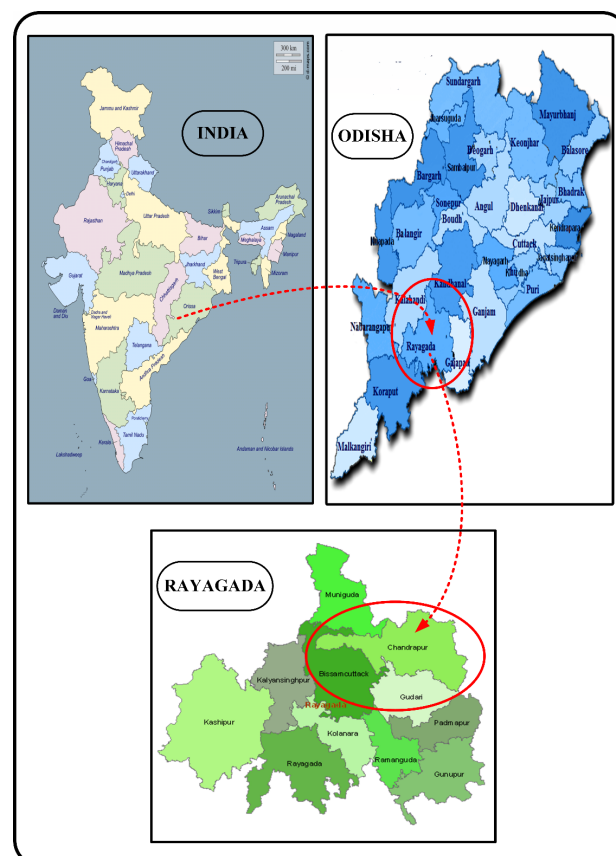

Figure 1. The position of the research region on the Indian map.

3. Renewable Energy Resources Identification in the Study Region

Natural RE resources can be exploited to electrify off-grid areas. The study area has been completely covered by solar and biomass energy resources. The study area's annual ambient temperature is 26 °C. The simulation used a ten-year average, i.e., from 2005 to 2015, of ambient temperature and solar radiation values obtained from the National Renewable Energy Laboratory, which are provided, respectively, in Figures 2 and 3. The study area is located in the middle of a high-density forest, which is around 196 hectares. With a foliage production assumption of 16 tons per hectare. Each year, the foliage for the 196 hectares of forest will be 31.36 tons. If the yearly foliage collecting rate is 60%, the annual foliage collection will be around 19 tons.
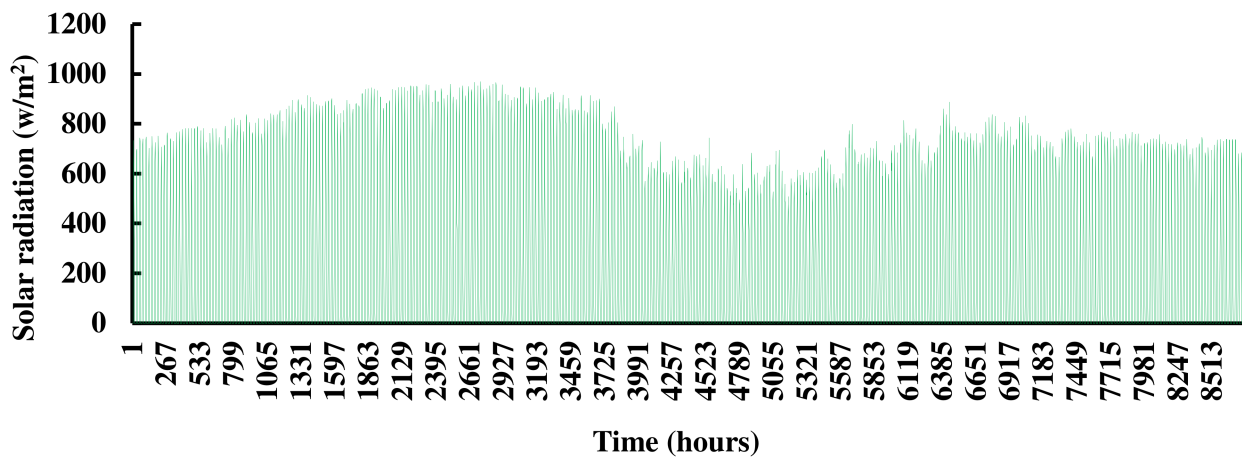
Figure 2. Study area's annual solar radiation.
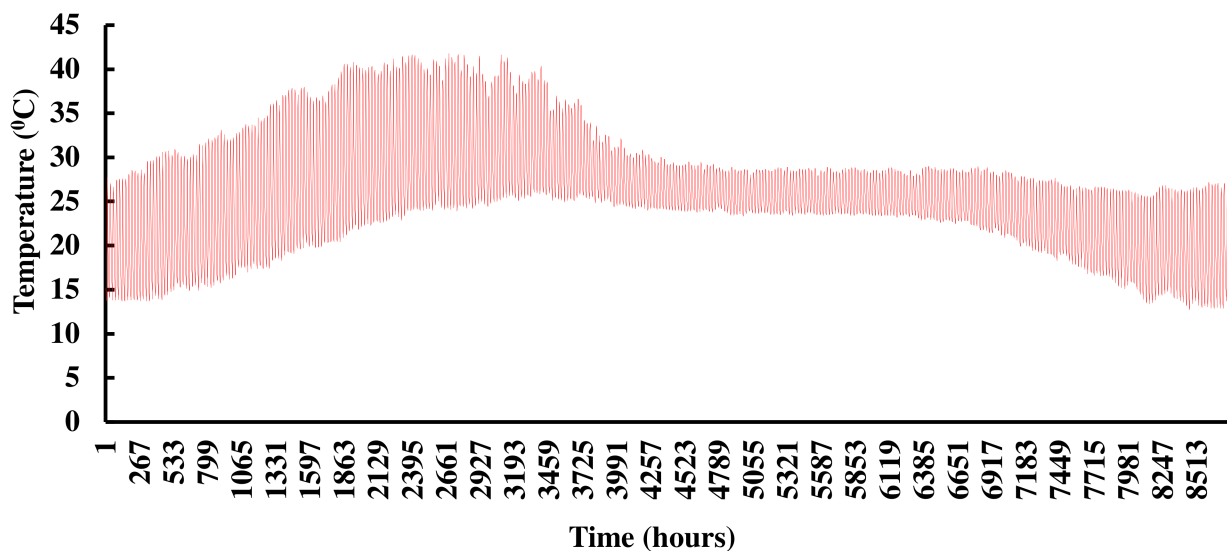
Figure 3. Study areas ambient temperature.

4. Study Area's Load Estimation

The load demands have been estimated based on the villagers' load requirements. According to villagers' needs, the total number of load sectors is anticipated to be domestic, community, agricultural, small scale industrial and commercial. Table 1 clearly explains the complete load estimation details of the rated power, quantity and time of usage of the appliances for the study areas winter (November–February) and summer (March–October) seasons of the study area. Figure 4 depicts the corresponding load demand graphs.

Table 1. Complete information on the study area's load demands.

Load Sector →	Domestic: LED Lamp	Domestic: Fan	Domestic: T.V+ Dish	Domestic: MC	School: LED Lamp	School: Fan	School: Computer	Hospital: LED Lamp	Hospital: Fan	Hospital: Refrigerator	Comm. Hall: LED Lamp	Comm. Hall: Fan	SL: LED Lights	PW: Motor (2 hp)	MCTM: Motor (5 hp)	Shops: LED Lamp	Shops: Fan	MDP: Motor (4 hp)	Flour Mill: Motor (5 hp)	SIL: Saw Machine	Hourly Energy Demand (kWh)
Rated Power →	20 W	75 W	100 W	5 W	20 W	75 W	250 W	20 W	75 W	200 W	20 W	75 W	40 W	1.5 kW	3.73 kW	20 W	75 W	2.983 kW	3.73 kW	1.8 kW	
Quantity →	2	1	1	1	12	12	12	5	5	1	3	3	27	6	1	5	5	3	1	1	
Time (h) ↓		S/W				S/W			S/W			S/W					S/W				S/W
0:00–1:00		11.48/0						0.1	0.38/0	0.2			0.6							12.76	12.76/0.9
1:00–2:00		11.48/0						0.1	0.38/0	0.2			0.6							12.76	12.76/0.9
2:00–3:00		11.48/0						0.1	0.38/0	0.2			0.6							12.76	12.76/0.9
3:00–4:00		11.48/0						0.1	0.38/0	0.2			0.6							12.76	12.76/0.9
4:00–5:00	3.06	11.48/0						0.1	0.38/0	0.2			0.6							15.82	15.82/3.96
5:00–6:00	3.06	11.48/0	3.83					0.1	0.38/0	0.2			0.6							19.65	19.65/7.79
6:00–7:00		11.48/0	3.83	0.77					0.38/0	0.2				4.5						21.16	21.16/9.30
7:00–8:00		11.48/0	3.83	0.77					0.38/0	0.2				4.5						21.16	21.16/9.30
8:00–9:00		11.48/0	3.83	0.38					0.38/0	0.2				4.5						20.77	20.77/8.91
9:00–10:00		5.74/0	3.83		0.24	0.9/0	3		0.38/0	0.2					3.73	0.1	0.38/0		1.8	20.30	20.30/12.90
10:00–11:00		5.74/0	3.83		0.24	0.9/0	3		0.38/0	0.2					3.73	0.1	0.38/0		1.8	20.30	20.30/12.90
11:00–12:00		5.74/0	7.65		0.24	0.9/0	3		0.38/0	0.2	0.06	0.23/0			3.73	0.1	0.38/0		1.8	24.41	24.41/16.78
12:00–13:00		5.74/0	7.65		0.24	0.9/0	3		0.38/0	0.2	0.06	0.23/0			3.73	0.1	0.38/0		1.8	24.41	24.41/16.78
13:00–14:00		5.74/0	7.65		0.24	0.9/0	3		0.38/0	0.2	0.06	0.23/0			3.73	0.1	0.38/0	3.73		26.34	26.34/18.71
14:00–15:00		5.74/0	7.65		0.24	0.9/0	3		0.38/0	0.2	0.06	0.23/0				0.1	0.38/0	3.73		22.61	22.61/14.98
15:00–16:00		5.74/0	7.65		0.24	0.9/0	3		0.38/0	0.2	0.06	0.23/0				0.1	0.38/0	3.73		22.61	22.61/14.98
16:00–17:00		5.74/0	7.65		0.24	0.9/0	3		0.38/0	0.2	0.06	0.23/0				0.1	0.38/0	3.73		22.61	22.61/14.98
17:00–18:00		5.74/0	7.65						0.38/0	0.2	0.06	0.23/0				0.1	0.38/0	3.73		18.47	18.47/11.74

Table 1. *Cont.*

Load Sector →	Domestic Load				Community Load								SL	Agricultural Load		Commercial Load				SIL	Hourly Energy Demand (kWh)
					School			Hospital			Community Hall			PW	MCTM	Shops		MDP	Flour Mill	Saw Mills	
Appliance	LED Lamp	Fan	T.V+ Dish	MC	LED Lamp	Fan	Computer	LED Lamp	Fan	Refrigerator	LED Lamp	Fan	LED Lights	Motor (2 hp)	Motor (5 hp)	LED Lamp	Fan	Motor (4 hp)	Motor (5 hp)	Saw Machine	
Rated Power →	20 W	75 W	100 W	5 W	20 W	75 W	250 W	20 W	75 W	200 W	20 W	75 W	40 W	1.5 kW	3.73 kW	20 W	75 W	2.983 kW	3.73 kW	1.8 kW	
Quantity →	2	1	1	1	12	12	12	5	5	1	3	3	27	6	1	5	5	3	1	1	
Time (h) ↓	S/W				S/W			S/W			S/W					S/W					S/W
18:00–19:00	6.12	11.48/0	15.3	0.77				0.1	0.38/0	0.2	0.06	0.23/0	0.6			0.1	0.38/0			35.72	35.72/23.25
19:00–20:00	6.12	11.48/0	15.3	0.77				0.1	0.38/0	0.2	0.06	0.23/0	0.6			0.1	0.38/0			35.72	35.72/23.25
20:00–21:00	6.12	11.48/0	15.3	0.38				0.1	0.38/0	0.2			0.6							34.56	34.56/22.7
21:00–22:00	6.12	11.48/0	15.3	0.38				0.1	0.38/0	0.2			0.6							34.56	34.56/22.7
22:00–23:00	3.06	11.48/0	7.65	0.38				0.1	0.38/0	0.2			0.6							23.85	23.85/11.99
23:00–24:00		11.48/0						0.1	0.38/0	0.2			0.6							12.76	12.76/0.9
Total Load Demand																					528.83/282.4

SIL = Small Industrial Load; MCTM = Multi Crop Threshing Machine; PW = Pumping Water; S/W = Summer/Winter; SL = Street Lighting; MDP = Mini Diary Plant; MC = Mobile Charger".
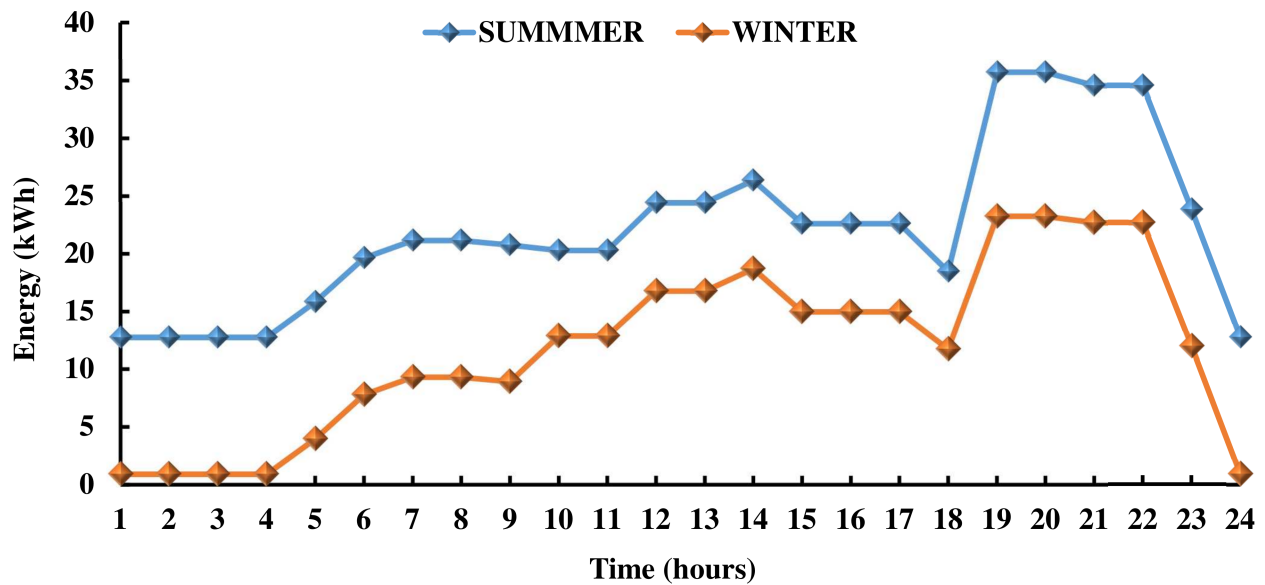
Figure 4. The daily load demand of the study area.

5. The Components of Mathematical Modelling

The optimal sizing of an off-grid microgrid is primarily determined by the components utilized in the analysis, hence accurate component analysis is essential before optimal sizing of the off-grid microgrid. The current study includes PV panels, a biomass generator, a battery bank and a bi-directional converter with a charge controller. The schematic diagram is shown in Figure 5.

5.1. Solar Energy System

A variety of approaches can be used to compute the PV output power from the PV panels. A normal framework was employed in this study to compute the output power of the PV panels, which was determined by taking into consideration of hourly ambient temperature and solar radiation values [14]:

$$P_{PV}(t) = PV_{rated} \times (G(t)/G_{ref}) \times \left[1 + K_T \times \left(T_C - T_{ref}\right)\right] \qquad (1)$$

where, T_{ref} = the standard test condition temperature value i.e., 25° degrees Celsius for PV cells. PV_{rated} = the PV panel's rated power, K_T = at maximum power, the temperature coefficient, its value is 3.7×10^{-3} (1/°C) and G_{ref} = the solar radiation value at reference condition, its value is 1000 W/m$^{2.}$.

The PV panel cell temperature (T_C) can be determined as:

$$T_C = T_{amb}(t) + (0.0256 \times G(t)) \qquad (2)$$

The amount of energy produced by the PV panels (E_{PV}) can be determined as follows:

$$E_{PV}(t) = N_{PV} \times P_{PV}(t) \times \Delta t \qquad (3)$$

where, Δt = time period.
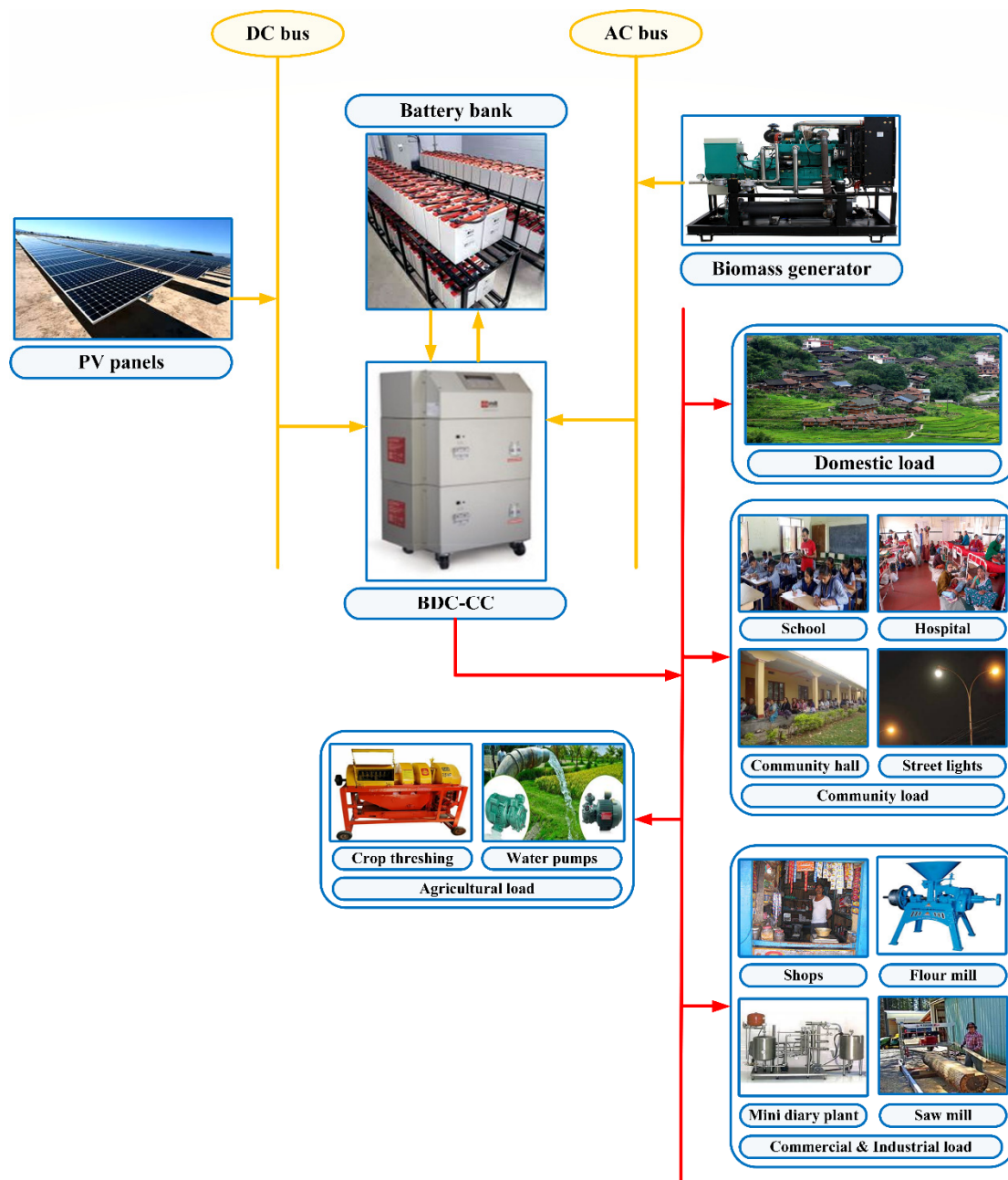
Figure 5. Schematic diagram of the study area electrification model.

5.2. Biomass Generator

In this study, we are advised to use the down draught gasifier model of biomass generator. The following equation can be used to calculate the power generated by the Biomass Generator [1]:

$$P_{BMG}(t) = \frac{Q_{BM} \times \eta_{BMG} \times CV_{BM} \times 1000}{DOH_{BMG} \times 365 \times 860} \qquad (4)$$

where, the conversion factor from kcal to kWh is 860, Q_{BM} = biomass quantity (tons/year), η_{BMG} = efficiency of the biomass generator, DOH_{BMG} = per day operative hours of the biomass generator and CV_{BM} = the biomass has a calorific value of 4015 kcal/kg.

The biomass generator's hourly energy output is determined as follows:

$$E_{BMG}(t) = P_{BMG}(t) \times \Delta t \qquad (5)$$

5.3. Battery Bank

When RE sources are not available to deliver power, the battery bank will supply power in off-grid systems. In general, the battery bank stores the extra energy generated by the RE sources. This phenomenon is known as a battery bank charging process, and it is expressed by the equation below [14,15]:

$$E_{Bat}(t) = (1 - \sigma) \times E_{Bat}(t-1) + (E_G(t) - E_L(t)/\eta_{Conv}) \times \eta_{CC} \times \eta_{rbat} \tag{6}$$

where, $E_{Bat}(t)$, and $E_{Bat}(t-1)$ are the energy levels of a battery bank, respectively, at time "$t-1$" and "t", σ = hourly self-discharge rate of the battery, η_{CC} = efficiency of the charge controller, E_L = electrical energy demand, E_G = generated electrical energy, η_{Conv} = the bidirectional converter's efficiency and η_{rbat} = the battery's round-trip efficiency.

The total electrical energy generation is calculated as:

$$E_G(t) = [E_{DC}(t) + E_{AC}(t)] \times \eta_{Conv} \tag{7}$$

where, (E_{DC}) denotes the DC energy produced by the RE resources:

$$E_{DC}(t) = E_{PV}(t) \tag{8}$$

The AC energy (E_{AC}) produced by RE sources is calculated as follows:

$$E_{AC}(t) = E_{BMG}(t) \tag{9}$$

Whenever the energy produced by the RE sources is inadequate to meet the load demands or when RE resources completely fail to meet the load demand. The energy in the battery bank will supply the load demand; this occurrence is known as the battery bank discharge process, and it is described in the following equation:

$$E_{Bat}(t) = (1 - \sigma) \times E_{Bat}(t-1) - (E_L(t)/\eta_{Conv} - E_G(t))/\eta_{rbat} \tag{10}$$

5.4. Bi-Directional Converter with a Charge Controller

The bi-directional converter is essential in off-grid systems because it collects energy from both DC and AC sources. Its primary function is to convert direct current to alternating current and vice versa. The charge controller inside the converter is useful for controlling the battery bank's overcharging and discharging. The following equation can be used to compute the converter's rated power for the off-grid microgrid [2]:

$$P_{BDC-CC} = E_{T,max} \times 1.1 \tag{11}$$

The multiplication factor 1.1 specifies the converter's overloading capacity, which means that the converter power rating should be 10% greater than the system's peak load demand.

6. Economic Analysis of the Off-Grid Microgrid

The Life Cycle Cost (LCC) technique is widely used for economic analysis. The LCC has been estimated in this study by adding the Initial Capital Costs (ICC), Erection Costs (*EREC*), the Present Value of O&M Costs ($P_{V,O\&M}$), the Present Value of Replacement Costs ($P_{V,REP}$) and the Present Value of Fuel Costs ($P_{V,FUEL}$) using all system components, which is expressed as follows [2]:

$$LCC = ICC + EREC + P_{V,O\&M} + P_{V,REP} + P_{V,FUEL} \tag{12}$$

The initial capital cost (*ICC*) of the IRES components are calculated as follows [2]:

$$ICC = \begin{bmatrix} (C_{BMG,cap}) + (N_{PV} \times C_{PV,cap}) + \\ (N_{BAT} \times C_{BAT,cap}) + (C_{BDC-CC,cap}) \end{bmatrix} \tag{13}$$

where, $C_{BMG,cap}$, $C_{PV,cap}$, $C_{BAT,cap}$ and $C_{BDC-CC,cap}$ are the initial capital costs of the biomass generator, PV panels, batteries and bi-directional converter with a charge controller respectively.

The erection costs (*EREC*) of the IRES components are calculated as follows [2]:

$$EREC = \begin{bmatrix} (N_{PV} \times C_{PV,erect}) + \left((N_{BAT} \times C_{BAT,erect}) \times \sum_{b=1}^{N_r} \frac{(1+x)^{bN_c-1}}{(1+y)^{bN_c}} \right) + \\ \left(C_{BDC-CC,erect} \times \sum_{d=1}^{N_r} \frac{(1+x)^{dN_c-1}}{(1+y)^{dN_c}} \right) + \left(C_{BMG,erect} \times \sum_{g=1}^{N_r} \frac{(1+x)^{gN_c-1}}{(1+y)^{gN_c}} \right) \end{bmatrix} \quad (14)$$

where, $C_{PV,erect}$, $C_{BAT,erect}$, $C_{BDC-CC,erect}$ and $C_{BMG,erect}$ are erection costs of the PV panels, batteries and bi-directional converter with a charge controller and biomass generator, respectively.

The present value of annual O&M ($P_{V,O\&M}$) costs of the IRES components are calculated as follows [2]:

$$P_{V,O\&M} = \begin{bmatrix} (N_{PV} \times C_{PV,o\&m}) + (C_{BMG,o\&m}) \\ (N_{BAT} \times C_{BAT,o\&m}) + (C_{BDC-CC,o\&m}) \end{bmatrix} \times \sum_{i=1}^{N} \frac{(1+x)^{i-1}}{(1+y)^i} \quad (15)$$

where, $C_{PV,o\&m}$, $C_{BMG,o\&m}$, $C_{BAT,o\&m}$ and $C_{BDC-CC,o\&m}$ are O&M costs of the PV panels, biomass generator, batteries and bi-directional converter with a charge controller, respectively, and y is defined as follows [2]:

$$y = \frac{I_{nom} - x}{1+x}. \quad (16)$$

where, I_{nom} = nominal interest rate, y = discount rate, N = life span of the project and x = inflation rate of the project.

The IRES components, such as a bi-directional converter with a charge controller, biomass generator are needed to replace because they have a shortened lifespan than the project lifetime. The present value of annual replacement cost ($P_{V,REP}$) of the microgrid is calculated as follows [2]:

$$P_{V,REP} = \begin{bmatrix} \left(N_{BAT} \times C_{BAT,rep} \times \sum_{b=1}^{N_r} \frac{(1+x)^{bN_c-1}}{(1+y)^{bN_c}} \right) + \left(C_{BMG,rep} \times \sum_{g=1}^{N_r} \frac{(1+x)^{gN_c-1}}{(1+y)^{gN_c}} \right) + \\ + \left(C_{BDC-CC,rep} \times \sum_{d=1}^{N_r} \frac{(1+x)^{dN_c-1}}{(1+y)^{dN_c}} \right) \end{bmatrix} \quad (17)$$

where, $C_{BAT,rep}$, $C_{BMG,rep}$ and $C_{BDC-CC,rep}$ are the replacement costs of the batteries, biomass generator and bi-directional converter with a charge controller, respectively, and the N_r is defined as follows [2]:

$$N_r = int\left(\frac{N - N_c}{N_c} \right) \quad (18)$$

where, N_r = the number of replacements needed for the system components and N_c = life span of each system component.

The present value of annual fuel cost ($P_{V,FUEL}$) of the microgrid is calculated as follows [2]:

$$P_{V,FUEL} = [(C_{BM} \times Q_{BM})] \times \sum_{i=1}^{N} \frac{(1+x)^{i-1}}{(1+y)^i} \quad (19)$$

where, Q_{BM} and C_{BM} are the quantity and cost of the biomass.

7. The Objective Function and Its Constraints

The objective function of the system is finding the optimal Life Cycle Cost (LCC) of the system. The system cost mainly depends on two variable parameters such as the number of PV panels and batteries. The objective function is defined as follows:

$$min \; LCC(N_{PV}, N_{BAT}) = \sum_{C=PV,BMG,BAT,BDC-CC}^{min} (LCC)_C \tag{20}$$

7.1. Upper and Lower Bounds

In this study, the biomass generator is considered as a fixed energy resource. Which is operational every day for 5 h, i.e., from 6 p.m. to 10 p.m. The biomass generator's rated power is considered to be 10 kW. The biomass generator produces around 9 kWh of energy each hour. As a result, the biomass generator is not bound by any constraints. PV energy is the remaining energy resource, which is bound by the following constraint.

$$1 \leq N_{PV} \leq N_{PV-max} \tag{21}$$

where, N_{PV} is the number of PV panels.

The battery bank is bound by the following constraint.

$$1 \leq N_{BAT} \leq N_{BAT-max} \tag{22}$$

where, N_{BAT} is the number of batteries.

7.2. Battery Bank Energy Storage Limits

During the charging and discharging processes, some energy will be stored or discharged from the battery bank, which will be limited by the following constraints [3]:

$$E_{Bat\_min} \leq E_{Bat}(t) \leq E_{Bat\_max} \tag{23}$$

The battery bank's min-max energy storage levels are computed as follows:

$$E_{Bat\_max} = \left(\frac{N_{BAT} \times V_{BAT} \times S_{BAT}}{1000} \right) \times SOC_{max-bat}. \tag{24}$$

$$E_{Bat\_min} = \left(\frac{N_{BAT} \times V_{BAT} \times S_{BAT}}{1000} \right) \times SOC_{min-bat} \tag{25}$$

where, S_{BAT} = rated capacity of the battery (Ah) and V_{BAT} = battery's voltage.

The battery's min-max state of charges are computed as follows:

$$SOC_{min-bat} = 1 - DOD \tag{26}$$

$$SOC_{max-bat} = SOC_{min-bat} + DOD \tag{27}$$

where, *DOD* is the depth of discharge of the battery.

7.3. Power Reliability Index

A microgrid's power reliability can be described as its capacity to supply power on a continuity basis. The *LPSP* is a critical microgrid criterion that will define the microgrid's power supply continuity. Which is calculated as follows [4]:

$$LPSP = \frac{\sum_{t=1}^{T} LPS(t)}{\sum_{t=1}^{T} E_L(t)} \tag{28}$$

where, $LPS(t)$ is the loss of power supply at any hour "*t*"

$$LPS(t) = \frac{E_L(t)}{\eta_{Conv}} - E_G(t) - [(1 - \sigma) \times E_{Bat}(t - 1) - E_{Bat\_min}] \times \eta_{rbat} \qquad (29)$$

8. Methodology

The methodology of the power flow among the various components used in the study are explained in the following modes of operation [5]:

Mode 1: In this operating mode, the power produced by the RE sources is equal to the load demand, hence there is no deficit or excess energy in the system.

Mode 2: In this operating mode, whenever the RE sources generate excess energy, it will be stored in the battery bank through the charging process of the battery bank.

Mode 3: In this operating mode, both the energy generated by the RE resources and the energy stored in the bank are at their maximum capacity. At this time, the extra energy generated will be delivered to the dump load.

Mode 4: This mode of operation demonstrates that whenever the energy provided by the RE resources is insufficient to supply the load demand, the energy stored in the battery bank will be delivered to the loads through the discharging process of the battery bank.

Mode 5: In this operating mode, the energy provided by the RE resources does not meet the load demand and the battery bank is also at its minimum energy storage levels, resulting in a loss of power supply to the system.

The above-mentioned modes of operation are depicted pictorially in the form of a flowchart as shown in Figures 6 and 7.

"Start

Read input data:
Yearly solar radiation, ambient temperature, biomass foliage,
electricity demand, fresh water demand and technical data of the components

Take one configuration out of the following twelve configurations:
PVP/BIOMG/BATTERY(Ni-Fe), PVP/BIOMG/BATTERY(Li-Ion) and
PVP/BIOMG/BATTERY(LA));

$E_{DC}(t) = E_{PV}(t)$; if with BMG based IHRES → $E_{AC}(t) = E_{BMG}(t)$;
if without BMG based IHRES → $E_{AC}(t) = 0$; $E_G(t) = E_{DC}(t) + E_{AC}(t)$;

for t=1:8760

$E_{net}(t) = E_G(t) - E_L(t)$

YES $E_{net}(t) \geq 0$ **A**

NO

$E_{dch}(t) = E_L(t) - E_G(t)$

Mode-5
Loss of power
supply

$E_{Bat}(t-1) - E_{Bat\_min} \geq E_{dch}(t)$ **NO**

Mode-4
Discharging
process

YES

$E_{Bat}(t) = E_{Bat\_min}$

$E_{Bat}(t) = (1-\sigma) \times E_{Bat}(t-1) - E_{dch}(t)/\eta_{rbat}$

$LPS(t) = E_L(t) - E_G(t)$

$LPS(t)=0$

$E_{Load\_supplied}(t) = E_G(t)$

$E_{Load\_supplied}(t) = E_L(t)$

Return

Return

B   End of
for loop

LPSP = sum of LPS in 8760 hours/sum of load
demand in 8760 hours"

Figure 6. Modes of operation for the off-grid microgrid.

"A"

$E_{net}(t) = 0$

Mode-3 Dump loading process

$E_{ch}(t) = E_G(t) - E_L(t)$

YES

Mode-1

$E_{ch}(t) \leq E_{Bat\_max} - E_{Bat}(t-1)$

$E_{Bat}(t) = E_{Bat}(t-1)$

NO

$E_{Bat}(t) = E_{Bat\_max}$

YES

Mode-2 Charging process

$LPS(t)=0$

$E_{dump}(t) = E_{ch}(t) - (E_{Bat\_max} - E_{Bat}(t-1))$

$E_{Bat}(t) = (1-\sigma) \times E_{Bat}(t-1) + E_{ch}(t) \times \eta_{CC} \times \eta_{rbat}$

$LPS(t)=0$

$LPS(t)=0$

$E_{Load\_supplied}(t) = E_L(t)$

$E_{Load\_supplied}(t) = E_L(t)$

$E_{Load\_supplied}(t) = E_L(t)$

Return

Return

Return

B"
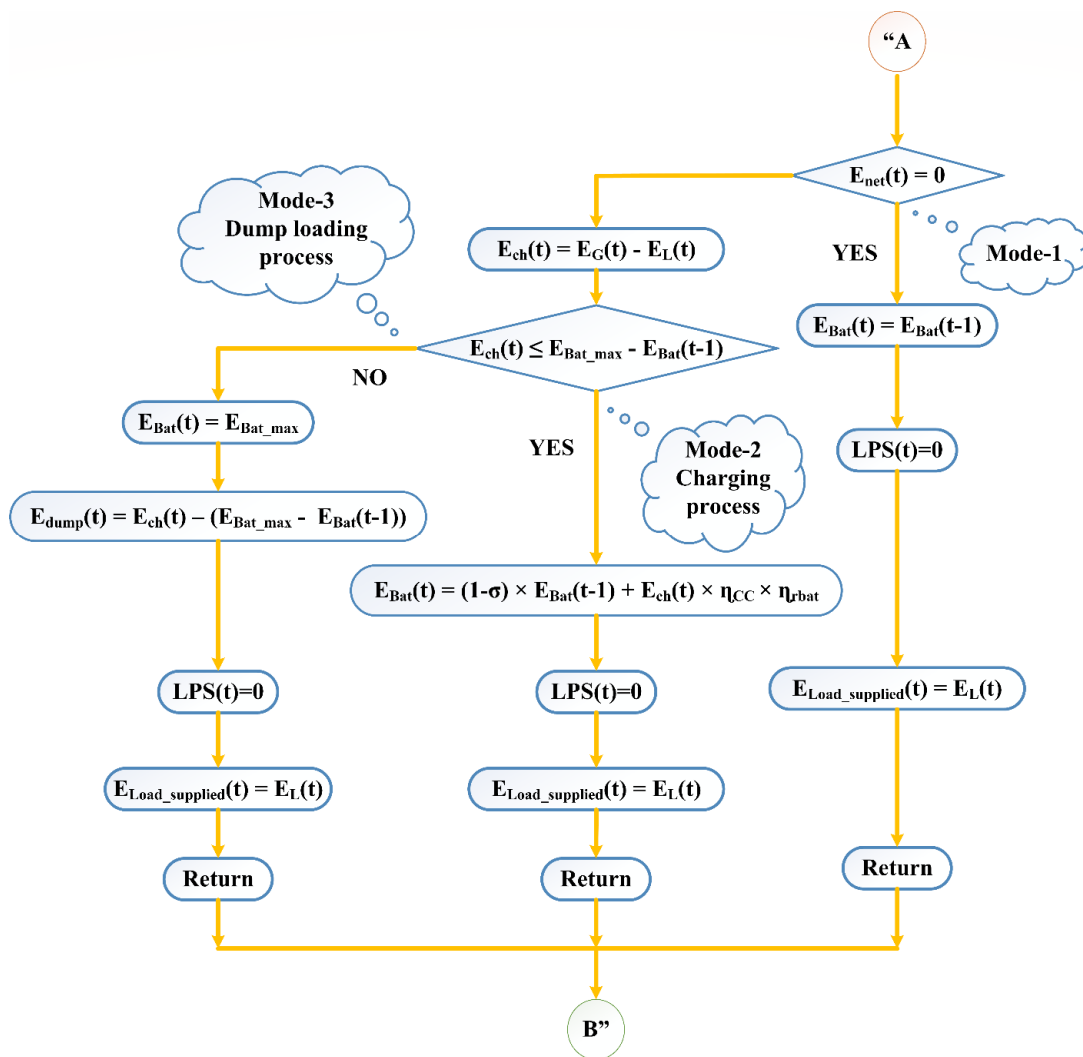
Figure 7. Modes of operation for the off-grid microgrid.

9. Results and Discussion

In general, using the existing RE resources, rural distant communities can be electrified. However, the fundamental disadvantage of RE resources is their inherent nature, as well as their energy production depends on the metrological conditions in the chosen location. As a result of the RE resources' time and metrological dependence, the power supply to the study area is not continuous.

As a result, while RE resources were used to electrify the study area, one of the key problems with these resources is that they cannot provide a continuous power supply. Hence, a reliable battery storage system is required to provide a continuous power supply. So, three different types of battery technologies have been proposed in this study to provide a continuous power supply in order to select a battery technology that is technologically and economically feasible for the study area.

Finally, we have been modelled three different types of configurations employing available RE resources and battery technologies, such as PVP/BIOMG/BATTERY$_{(Ni-Fe)}$, PVP/BIOMG/BATTERY$_{(Li-Ion)}$ and PVP/BIOMG/BATTERY$_{(LA)}$ to Identify a configuration that is technologically and economically feasible to electrify the study area. PV panels and batteries are the variable parameters in all of the three configurations and their quantities can be determined using optimization algorithms based on the required load demand and constraints. However, the biomass generator is regarded as a fixed energy resource, with a rated power of 10 kW. Hence, no optimization algorithm is required to estimate its

size because it is already fixed as a 10 kW. The converter size is also considered as a fixed parameter because it is already predesigned to meet the peak load demands of the study area. Because the study area's peak load demand is 35.72 kW, the converter power rating is set to 40 kW. For safety reasons, the converter power rating is set to be 10% higher than the peak load demand. As a result, there is no need to use optimization algorithms to optimize the converter size.

The three above-mentioned configurations have been optimized using well-known algorithms such as Differential Evolutionary Algorithm (DE) [10], Genetic Algorithm (GA) [11], Moth Flame Optimization (MFO) [12], Dragonfly Algorithm (DA) [13], Particle Swarm Optimization (PSO) [14], Ant Lion Optimization (ALO) [15], Grey Wolf Optimization (GWO) [16], Grasshopper Optimization Algorithm (GOA) [17] and Dynamic Differential Annealed Optimization Algorithm [18]. These algorithms that were run with their default control parameter values with the population and iterations are considered to be 100. The technical and cost values used in the study are listed in Tables 2 and 3.

Table 2. The study's technical and financial values.

Parameters	Value	Parameters	Value
Project lifetime	25 years	Erection cost of BIOMG [2]	450.5 USD
Nominal interest rate [2]	13%	Rated Power of BIOMG [6]	10 kW
Inflation rate [7]	5%	BIOMG Capital cost [6]	9010 USD
Manufacturer of PV Panel [19]	Vikram solar	AO&M cost of BIOMG [2]	$271
Model No. of PV Panel [19]	Somera 385	Quantity of biomass	19 tons/year
Rated power of PV Panel [19]	385 Wp	Cost of biomass [2]	15 USD/ton
Lifetime of PV Panel [8]	25 years	Efficiency of BIOMG [2]	20%
Capital cost of PV Panel [8]	128 USD	Rated power of BDC-CC	40 kW
AO&M cost of PV Panel [2]	3.2 USD	Lifetime of converter [2]	10 years
Mechanical structure cost of PV Panel [20]	41 USD	C&R of converter [2]	4320 USD
Life time of mechanical structure of PV panel [20]	25 years	AO&M cost of converter [2]	108 USD
Erection cost of PV panel [2]	25.6 USD	Efficiency of converter [2]	95%
Erection cost of battery [2]	3% of CC of battery	Erection cost of converter [2]	129.6 USD

Table 3. The study's technical and financial values of the batteries.

Battery Type	Lead Acid (PbSO$_4$)	Lithium Iron Phosphate (LiFePO$_4$)	Nickel Iron (Ni-Fe)
Manufacturer	Trojan [21]	Victron [22]	Iron Edison [23]
Model	SSIG 06 490	LFP-12.8/200-a	TN 1000
Nominal capacity (S_{BAT})	490 Ah	300 Ah	1000 Ah
Nominal voltage (V_{BAT})	6 V	12.8 V	1.2 V
Round trip efficiency (η_{rbat})	85%	92%	80%
Lifespan in years	2.5 years	15 years	30 years+
Self-discharge rate (%/day) (σ)	0.3%	0.2%	1%
Capital cost (CC) in USD	410	3317	1057
Annual O&M cost in USD	2.5% of CC	No maintenance	2% of CC
Operating temperature	−20 °C to +45 °C	−20 °C to +50 °C	−30 °C to +60 °C
Cycle life of the batteries	750 cycles	5000 cycles	11,000+ cycles

The results shown in Table 4 were obtained with an LPSP value of 0% for the above-mentioned three configurations using the algorithms shown above. For each configuration, this table shows the optimal LCC values as well as the optimal number of PV panels and batteries.

Table 4. Optimization results of all configurations at an LPSP value of 0%.

Configuration	Q&C	GA	PSO	DE	GWO	ALO	DA	MFO	GOA	DDAO
PVP/ BIOMG/ BATTERY(Ni-Fe)	N_{PV}	511	511	513	511	511	513	511	516	511
	N_{BAT}	351	351	351	351	352	352	351	352	351
	LCC in USD	367,586	367,586	368,088	367,586	368,153	368,655	367,586	369,407	367,586
	STIS	8687	8906	20538	8938	8980	9080	8806	8972	8152
PVP/ BIOMG/ BATTERY(LA)	N_{PV}	475	474	474	478	474	476	477	474	474
	N_{BAT}	136	136	136	136	136	137	136	136	136
	LCC in USD	607,281	607,030	607,030	608,032	607,030	610,821	607,781	607,030	607,030
	STIS	8871	8669	20820	9007	8980	9120	8889	8992	8083
PVP/ BIOMG/ BATTERY(Li-Ion)	N_{PV}	436	438	439	436	437	436	436	439	436
	N_{BAT}	155	155	157	155	155	155	155	156	155
	LCC in USD	1,019,683	1,020,185	1,031,657	1,019,683	1,019,934	1,019,683	1,019,683	1,026,046	1,019,683
	STIS	8814	8845	20542	8874	8834	8953	8792	8811	8092

9.1. The Impact of Various Battery Technologies on System Performance

According to the results given in Table 4, the configuration made up of Ni-Fe battery technology provided the lowest LCC value when compared to the configurations made up of LA and Li-Ion battery technologies. The Ni-Fe battery configuration offered the optimal LCC value as 367,586 USD and its required number of PV panels and Ni-Fe batteries to electrify the study area are 511 and 351, respectively.

The next optimal configuration to electrify the study area is the configuration made up of LA battery technology, which has provided the optimal LCC value as 607,030 USD, which is about 65% higher than the LCC value obtained with the Ni-Fe battery technology and about 41% lower than the LCC obtained with the Li-Ion battery technology. To electrify the study area using the configuration made up of LA battery technology, 474 PV panels and 136 LA batteries are required.

The final optimal configuration to electrify the study area is the configuration made up of Li-Ion battery technology, which produced the optimal LCC value as 1,019,683 USD. Which is about 177% and 68% higher than the LCCs obtained with the configurations made up of Ni-Fe and LA battery technologies, respectively. Finally, the number of PV panels and Li-Ion batteries required to electrify the study area with this configuration are 436 and 155, respectively.

Figure 8 depicts the annual energy production of the PV panels and biomass generator, as well as the charging and discharging process of the battery bank based on load demand.

9.2. Robustness of the Algorithms

The robustness of the algorithm can be determined by its ability to provide the global best optimal values for the proposed configurations. Three configurations were modelled in this study, and these configurations were tested using well-known algorithms as well as a new proposed metaheuristic algorithm Dynamic Differential Annealed Optimization (DDAO). For each of these three configurations, the proposed algorithm, DDAO, provided the optimal LCC values. The number of times each algorithm provided the global best optimal values for three configurations are shown in Table 5.
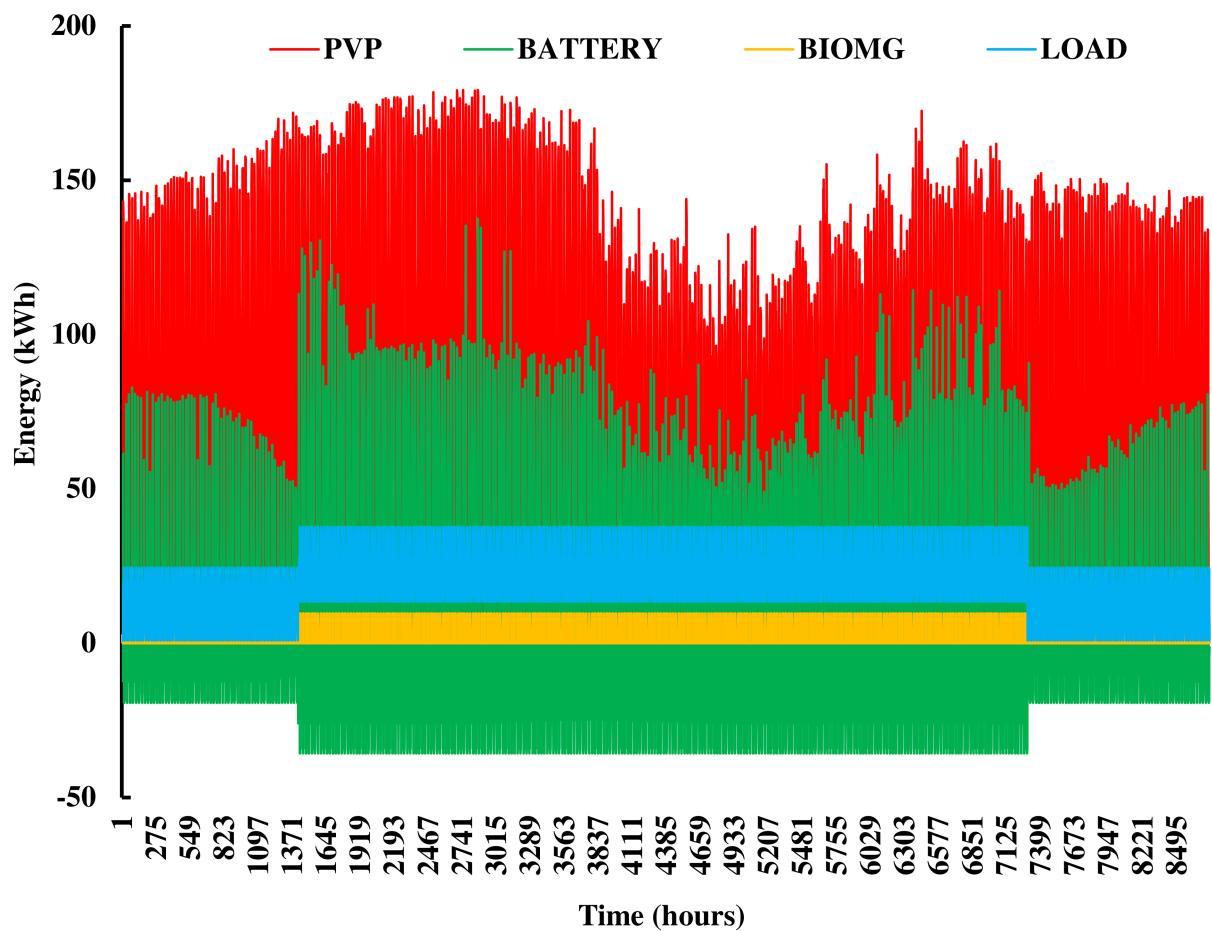
Figure 8. Energy output graph for different components of a Ni-Fe battery configuration over a year.

Table 5. Rankings of algorithms in providing the optimal values.

S.No.	Algorithms	Optimal Values Given Times	Ranking
1	DDAO	3	1
2	GA, PSO, GWO and MFO	2	2
3	DE, DA and GOA	1	3

According to Table 4, when compared to the remaining algorithms in terms of Simulation Time in Seconds (STIS), the DDAO algorithms performed the best in both finding global best optimal values and simulation completion process.

The convergence curves for the three configurations proposed in the study are depicted in Figures 9–11.

9.3. Loss of Power Supply Probability

The configuration made up of Ni-Fe battery technology is identified as the optimal configuration for electrifying the study area. This configuration was examined with various probabilities of power supply failure. As a result, the optimal configuration was examined with different LPSP values ranging from 1% to 5%. Table 6 shows the optimal values for this configuration with various LPSP values. Table 6 and Figure 12 shows that at the LPSP value of 1%, there is a significant change in all values when compared to the values obtained at the LPSP value of 0%. When we compare the difference between the 1% LPSP and the remaining LPSP values ranging from 2% to 5% optimal values, the difference in LCC and component values is not that much of significant. At an LPSP value of 1%, the

number of power supply hours lost is also 123 only out of 8760 h. As a result, electrification of the study area at an LPSP value of 1% is also recommendable.
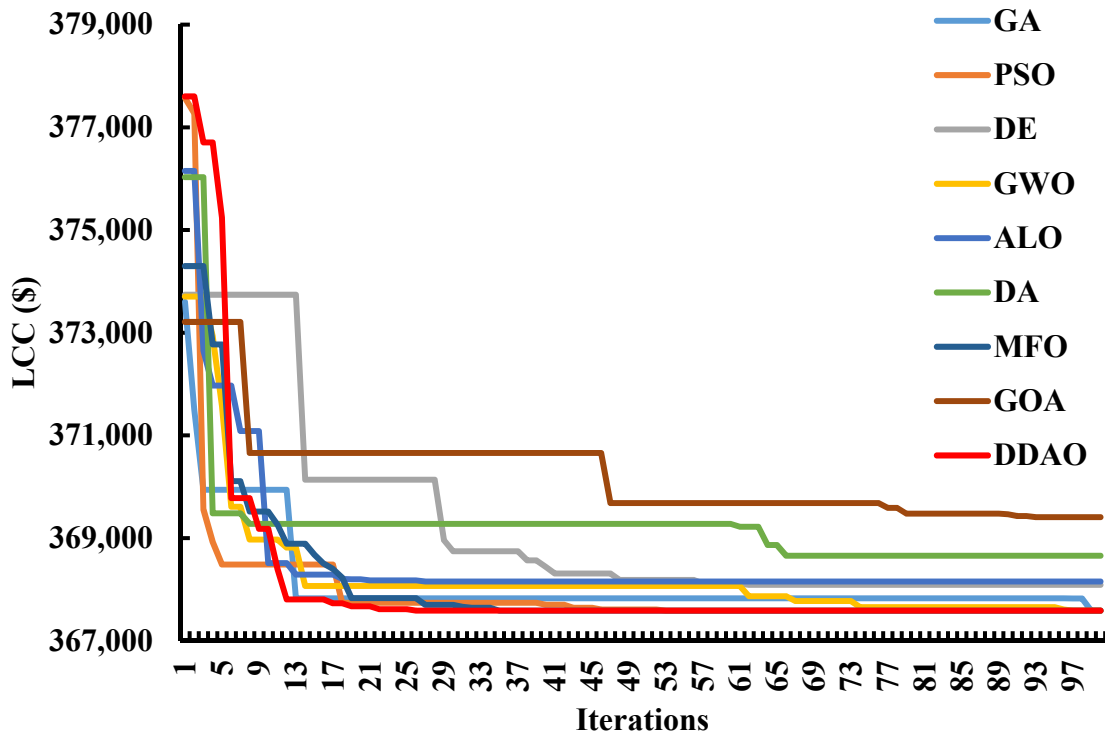
**Figure 9.** Convergence curves of the configuration made up of Ni-Fe battery.
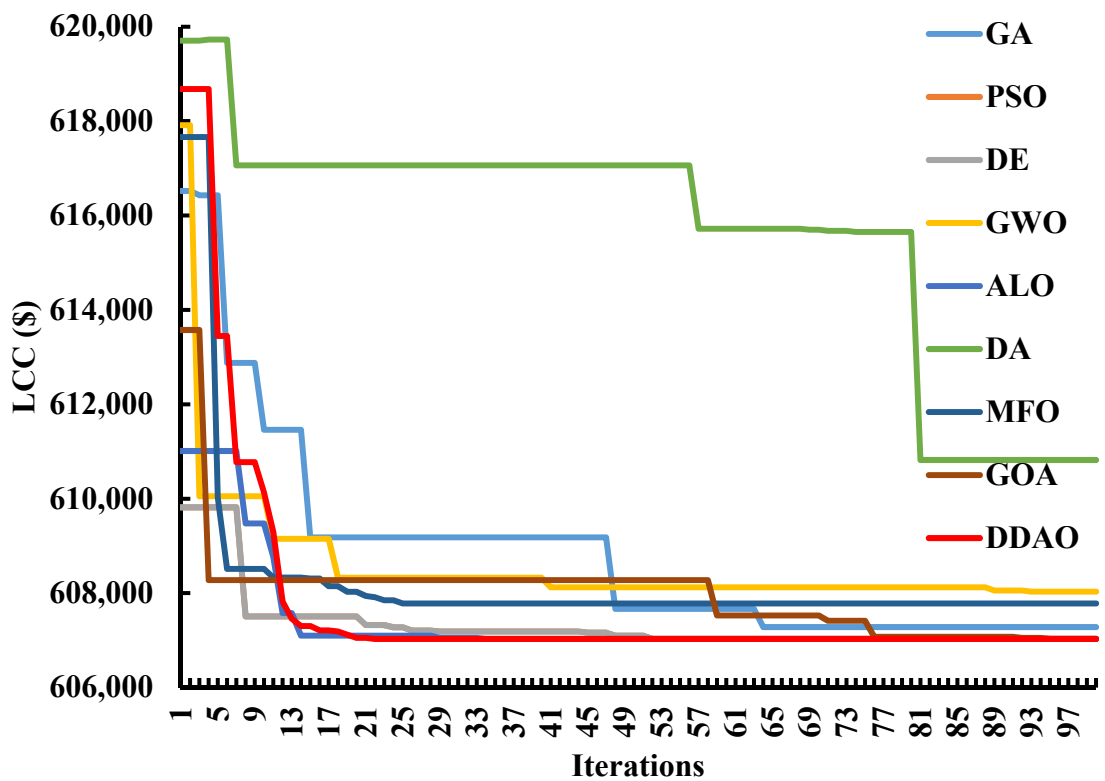
Figure 10. Convergence curves of the configuration made up of LA battery.
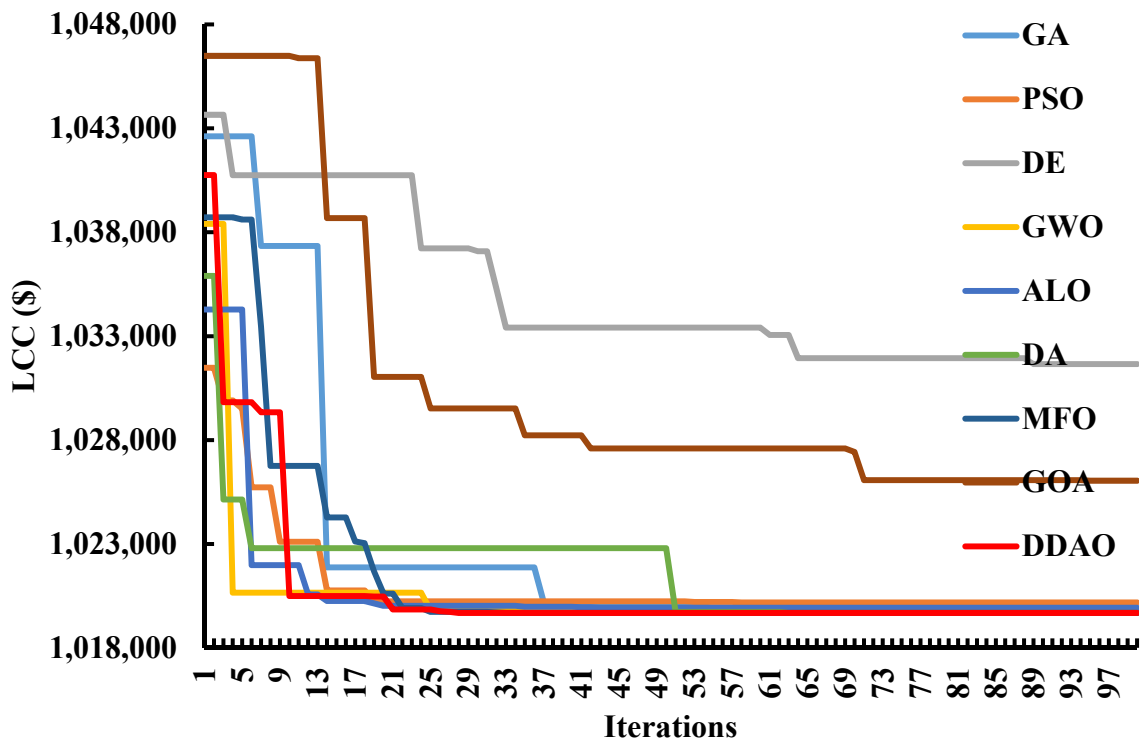
**Figure 11.** Convergence curves of the configuration made up of Li-Ion battery.
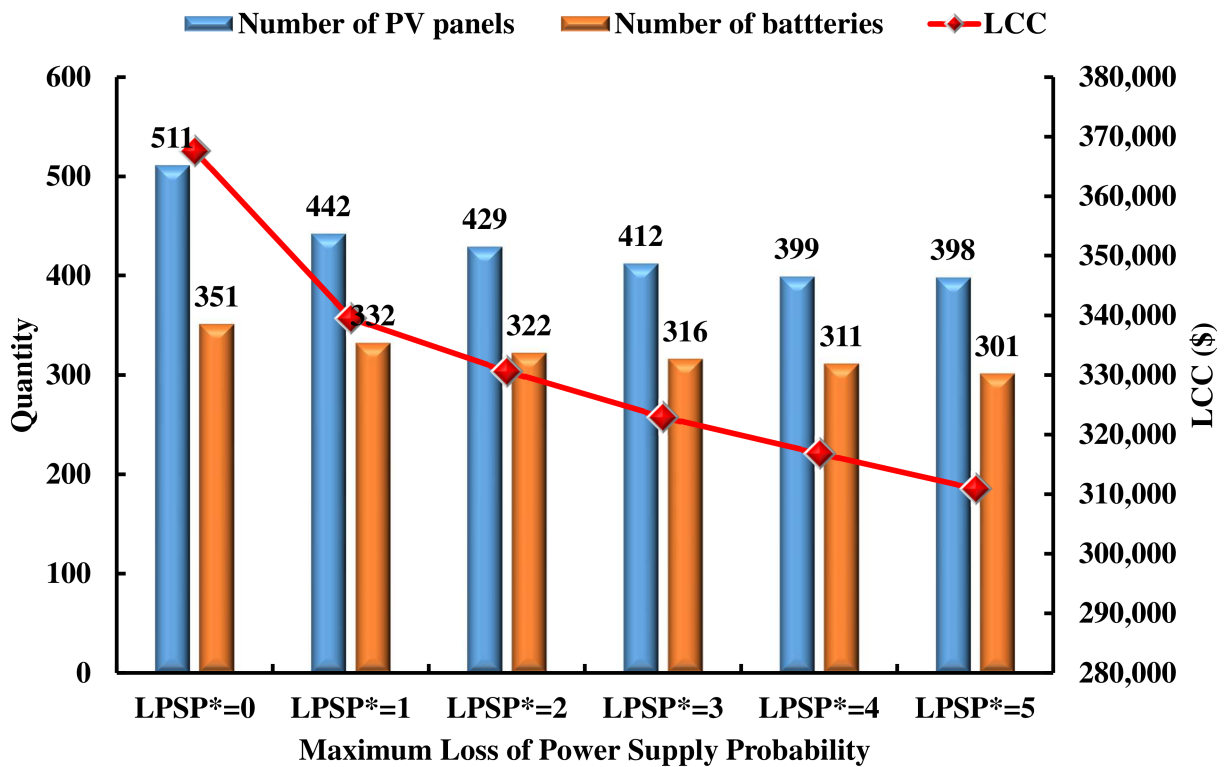
Figure 12. The Ni-Fe battery configuration analysis with different LPSP values.

Table 6. Optimum configuration results for various LPSP values.

Configuration	Quantity & Cost	LPSP (0%)	LPSP (1%)	LPSP (2%)	LPSP (3%)	LPSP (4%)	LPSP (5%)
PVP/ BIOMG/ BATTERY (Ni-Fe)	N_{PV}	511	442	429	412	399	398
	N_{BAT}	351	332	322	316	311	301
	LCC in USD	367,586	339,523	330,600	322,939	316,847	310,933
	LPSH	0	182	317	430	564	632

10. Conclusions

The current study has focused on off-grid rural electrification in a remote rural area of the Indian state of Odisha. The location is still not electrified due to its remote location because grid extension to that area is not feasible for two reasons: first, extending the grid to that area is more expensive because it is more than 50 km away. The second reason is that grid extension is not a viable option for the location since it is located in a densely forested area surrounded by hilly mountains. As a result, electrification of the study area is planned, utilizing the study area's readily available RE resources, such as solar and biomass. However, due to the time dependence and metrological weather conditions dependence of these RE resources, the power supply is not continuous. As a consequence, three different types of battery technologies have been proposed for the current study. To identify a battery technology that is technologically and economically suitable for the study area.

The current study used available RE resources and battery technologies to model three configurations: PVP/BIOMG/BATTERY$_{(Ni-Fe)}$, PVP/BIOMG/BATTERY$_{(Li-Ion)}$ and PVP/-BIOMG/BATTERY$_{(LA)}$. The main goal here is to identify the configuration that is appropriate for electrifying the study area. The identification process incorporated with nine well-known and established algorithms, such as Differential Evolutionary Algorithm, Genetic Algorithm, Moth Flame Optimization, Dragonfly Algorithm, Particle Swarm Optimization, Grey Wolf Optimization, Ant Lion Optimization, Grasshopper Optimization Algorithm and Dynamic Differential Annealed Optimization (DDAO) Algorithm. When DDAO was compared to the remaining algorithms, it produced the global best optimal results. Based on the results, the PVP/BIOMG/BATTERY$_{(Ni-Fe)}$ configuration was identified as the feasible configuration to electrify the study area.

When compared to the configurations made up of Li-Ion and LA battery, the configuration of Ni-Fe battery provided the lowest LCC value as 367,586 USD, which is 39% and 64% lower in percentage terms. The optimal configuration has been further analyzed with different loss of power supply probability values ranging from 1% to 5%. According to the findings, at a loss of power supply probability value of 1%, the optimal configuration may be recommendable for electrifying the study area.

Author Contributions: Conceptualization P.P.K.; methodology, P.P.K.; software, P.P.K.; validation, P.P.K. and M.J.; formal analysis, P.P.K.; investigation, P.P.K. and V.S.; resources, M.J. and V.S.; data curation, M.J. and P.P.K.; writing—original draft preparation, P.P.K.; writing—review and editing, M.J. and V.S.; visualization, P.P.K., V.S. and M.J.; supervision, Z.L.; project administration, Z.L.; funding acquisition, Z.L, V.S. and M.J. All authors have read and agreed to the published version of the manuscript.

Data Availability Statement: Not Applicable.

Conflicts of Interest: No conflict of Interest.

References

1. Patel, A.M.; Singal, S.K. Optimal component selection of integrated renewable energy system for power generation in stand-alone applications. *Energy* **2019**, *175*, 481–504. [CrossRef]
2. Man, K.F.; Tang, K.S.; Kwong, S. Genetic algorithms: Concepts and applications. *IEEE Trans. Ind. Electron.* **1996**, *43*, 519–534. [CrossRef]
3. Kumar, P.; Saini, R.P. Optimization of an off-grid integrated hybrid renewable energy system with various energy storage technologies using different dispatch strategies. *Energy Sources Part A Recovery Util. Eff.* **2020**, *32*, 1–30. [CrossRef]
4. Kumar, P.P.; Saini, R.P. Optimization of an off-grid integrated hybrid renewable energy system with different battery technologies for rural electrification in India. *J. Energy Storage* **2020**, *32*, 101912. [CrossRef]
5. Salameh, T.; Kumar, P.P.; Sayed, E.T.; Abdelkareem, M.A.; Rezk, H.; Olabi, A.G. Fuzzy modeling and particle swarm optimization of Al_2O_3/SiO_2 nanofluid. *Int. J. Thermofluids* **2021**, *10*, 100084. [CrossRef]
6. Storn, R. Differential Evolution—A Simple and Efficient Heuristic for Global Optimization over Continuous Spaces. *J. Glob. Optim.* **1997**, *11*, 341–359. [CrossRef]
7. Mirjalili, S. Moth-flame optimization algorithm: A novel nature-inspired heuristic paradigm. *Knowl. Based Syst.* **2015**, *89*, 228–249. [CrossRef]
8. Mirjalili, S. Dragonfly algorithm: A new meta-heuristic optimization technique for solving single-objective, discrete, and multi-objective problems. *Neural Comput. Appl.* **2016**, *27*, 1053–1073. [CrossRef]
9. Kennedy, J.; Eberhart, R. Particle Swarm Optimization. In Proceedings of the ICNN'95-International Conference on Neural Networks, Perth, WA, Australia, 27 November–1 December 1995; pp. 1942–1948.
10. Mirjalili, S. The Ant Lion Optimizer. *Adv. Eng. Softw.* **2015**, *83*, 80–98. [CrossRef]
11. Mirjalili, S.; Mohammad, S.; Lewis, A. Grey Wolf Optimizer. *Adv. Eng. Softw.* **2014**, *69*, 46–61. [CrossRef]
12. Saremi, S.; Mirjalili, S.; Lewis, A. Advances in Engineering Software Grasshopper Optimisation Algorithm: Theory and Application. *Adv. Eng. Softw.* **2017**, *105*, 30–47. [CrossRef]
13. Ghafil, H.N.; Jármai, K. Dynamic differential annealed optimization: New metaheuristic optimization algorithm for engineering applications. *Appl. Soft Comput. J.* **2020**, *93*, 106392. [CrossRef]
14. Bukar, A.L. Optimal sizing of an autonomous photovoltaic/wind/battery/diesel generator microgrid using grasshopper optimization algorithm. *Solar Energy* **2019**, *188*, 685–696. [CrossRef]
15. Chauhan, A.; Saini, R.P. Discrete harmony search based size optimization of Integrated Renewable Energy System for remote rural areas of Uttarakhand state in India. *Renew. Energy* **2016**, *94*, 587–604. [CrossRef]
16. Maleki, A. Design and optimization of autonomous solar-wind-reverse osmosis desalination systems coupling battery and hydrogen energy storage by an improved bee algorithm. *Desalination* **2018**, *435*, 221–234. [CrossRef]
17. Enersol Biopower. Available online: http://enersolbiopower.com/ (accessed on 5 May 2020).
18. Reserve Bank of India. Available online: https://www.rbi.org.in/home.aspx (accessed on 12 February 2020).
19. Vikram Solar. Available online: https://www.vikramsolar.com/ (accessed on 25 May 2020).
20. Mechanical Structure Cost of PV Panel. Available online: https://www.loomsolar.com/products/loom-solar-2-row-design-6-panel-stand-375-watt?gclid=CjwKCAjwsan5BRAOEiwALzomXxjAoKPGLLYkGRoWRgkR7mAros-FbPGeWeNhzvOqId-TRQESPrWq3xoC3CAQAvD_BwE (accessed on 12 May 2020).
21. Trojan Battery Company. Available online: https://www.trojanbattery.com/ (accessed on 12 January 2020).
22. Victron Energy Blue Power. Available online: https://www.victronenergy.com/batteries (accessed on 15 January 2020).
23. Iron Edison. Available online: https://ironedison.com/store (accessed on 10 January 2020).